

Effects of the Location of Distal Histidine in the Reaction of Myoglobin with Hydrogen Peroxide*

(Received for publication, July 27, 1998, and in revised form, November 3, 1998)

Toshitaka Matsui^{‡§}, Shin-ichi Ozaki[‡], Elaine Liong[¶], George N. Phillips, Jr.[¶],
and Yoshihito Watanabe^{‡||**}

From the [‡]Institute for Molecular Science and the ^{||}Department of Structural Molecular Science, Graduate University for Advanced Studies, Myodaiji, Okazaki 444, Japan and the [¶]Department of Biochemistry and Cell Biology, Rice University, Houston, Texas 77251

To clarify how the location of distal histidine affects the activation process of H₂O₂ by heme proteins, we have characterized reactions with H₂O₂ for the L29H/H64L and F43H/H64L mutants of sperm whale myoglobin (Mb), designed to locate the histidine farther from the heme iron. Whereas the L29H/H64L double substitution retarded the reaction with H₂O₂, an 11-fold rate increase *versus* wild-type Mb was observed for the F43H/H64L mutant. The V_{max} values for 1-electron oxidations by the myoglobins correlate well with the varied reactivities with H₂O₂. The functions of the distal histidine as a general acid-base catalyst were examined based on the reactions with cumene hydroperoxide and cyanide, and only the histidine in F43H/H64L Mb was suggested to facilitate heterolysis of the peroxide bond. The x-ray crystal structures of the mutants confirmed that the distal histidines in F43H/H64L Mb and peroxidase are similar in distance from the heme iron, whereas the distal histidine in L29H/H64L Mb is located too far to enhance heterolysis. Our results indicate that the proper positioning of the distal histidine is essential for the activation of H₂O₂ by heme enzymes.

Peroxidase is a heme enzyme that catalyzes 1-electron oxidations of a variety of substrates (1, 2). The ferric enzyme is oxidized by H₂O₂ to yield a ferryl porphyrin cation radical (Fe^{IV}=O Por⁺) known as compound I in the first step of the catalytic cycle (3). Compound I is reduced to the ferric state through a ferryl species (Fe^{IV}=O Por), so-called compound II, by two sequential 1-electron oxidations of substrates. The invariant histidine in the distal heme pocket (1–6) is a critical residue for peroxidases, and its replacement by aliphatic residues retards compound I formation by 5–6 orders of magnitude (7–9). As shown in Scheme I, the distal histidine is believed to function (i) as a general base to accelerate binding of H₂O₂ to the ferric heme iron by deprotonating the peroxide and (ii) as a general acid to facilitate the heterolytic cleavage of the O–O

bond of a plausible Fe^{III}-OOH complex by protonating the terminal oxygen atom (10). The charge separation in heterolysis is suggested to be also enhanced by a positively charged distal arginine (Scheme I), whose substitution results in 2 orders of magnitude slower formation of compound I (10–12).

Myoglobin (Mb),¹ a carrier of molecular oxygen, similarly possesses a distal histidine (His-64) in the heme pocket (Fig. 1) and can catalyze various oxidation reactions using H₂O₂ (13–19). However, Mb reacts with H₂O₂ much slower (~10² M⁻¹ s⁻¹) than peroxidases (~10⁷ M⁻¹ s⁻¹) to afford ferryl Mb (Mb-II) paired with a transient protein radical (Scheme II). Compound I of wild-type Mb (Mb-I) has not been observed and is considered to decay to Mb-II immediately (Scheme II). The poor reactivity of Mb with H₂O₂ might be partly due to the malfunction of the distal histidine as a general acid-base catalyst and the absence of the distal arginine. Whereas the distal histidine in peroxidase is suggested to raise the basicity of imidazole by a hydrogen bond with the adjacent asparagine (20, 21), the absence of the hydrogen bond in Mb (13, 14) is indicative of less basicity of its distal histidine. Furthermore, wild-type Mb cleaves the O–O bond of the heme-bound peroxide not only heterolytically, but also homolytically to give Mb-II and a hydroxy radical as shown in Scheme II (22–24). It has been suggested that the distal histidine in Mb is unable to enhance heterolysis as a general acid (25); however, the structural factor for this inability is still obscure.

Comparison of crystal structures of sperm whale Mb and horseradish peroxidase led us to propose that the distal histidine in Mb is too close to the heme center to enhance heterolysis as a general acid catalyst (Fig. 1) (14, 26). The distances between N^ε of the distal histidine and the ferric heme iron are normally 4.1–4.6 Å for globins (4.3 Å for sperm whale Mb) and 5.5–6.0 Å for peroxidases (6.0 and 5.6 Å for horseradish peroxidase and cytochrome *c* peroxidase, respectively) (6, 14, 26). To examine our hypothesis, we have studied the reactions of ferric wild-type, L29H/H64L, and F43H/H64L sperm whale Mb with H₂O₂ because the estimated iron-distal histidine distances for the L29H/H64L and F43H/H64L mutants are 6.6 and 5.4 Å, respectively (27, 28). The functions of distal histidines as general acids and general bases are examined based on the ratio of heterolysis *versus* homolysis of the O–O bond in cumene hydroperoxide and association rate constants of cyanide and azide, respectively. The F43H/H64L mutant shows the highest reactivity with H₂O₂, and its distal histidine functions as a general acid-base catalyst most efficiently. Furthermore, the x-ray crystal structures of the double mutants in this report confirm that the distal histidine in F43H/H64L Mb is at a

* This work was supported in part by a grant-in-aid for priority areas, molecular biometallics (to Y. W.); Robert A. Welch Foundation Grant C-1142, National Institutes of Health Grant AR40252, and Texas Advanced Technology Program Grant 003604-025 (to G. N. P.); and the W. M. Keck Center for Computational Biology. The costs of publication of this article were defrayed in part by the payment of page charges. This article must therefore be hereby marked "advertisement" in accordance with 18 U.S.C. Section 1734 solely to indicate this fact.

The atomic coordinates (codes 10FJ and 10FK) have been deposited in the Protein Data Bank, Brookhaven National Laboratory, Upton, NY.

§ Supported by research fellowships from the Japan Society for the Promotion of Science for Young Scientists.

** To whom correspondence should be addressed: Inst. for Molecular Science, Myodaiji, Okazaki 444, Japan. Tel.: 81-564-55-7430; Fax: 81-564-54-2254; E-mail: yoshi@ims.ac.jp.

¹ The abbreviations used are: Mb, myoglobin; Mb-I, compound I of Mb; Mb-II, compound II of Mb; HPLC, high pressure liquid chromatography; *m*CPBA, *m*-chloroperbenzoic acid; CHP, cumene hydroperoxide.

SCHEME I. Proposed mechanism for the formation of compound I.

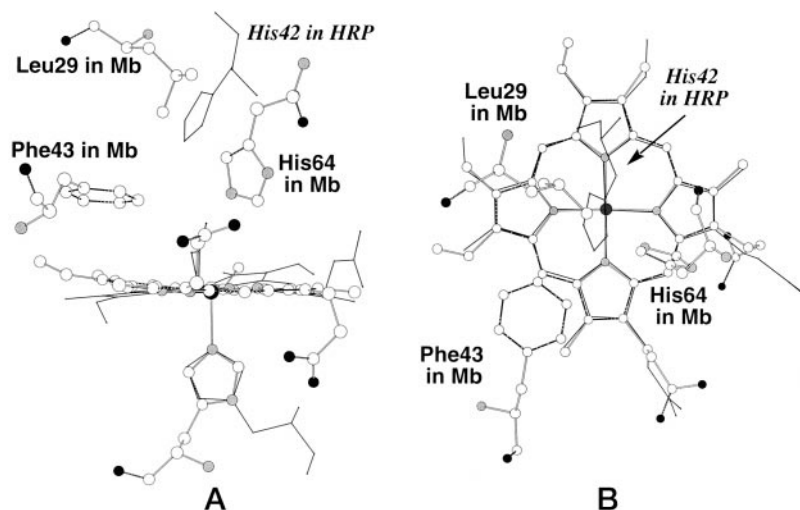
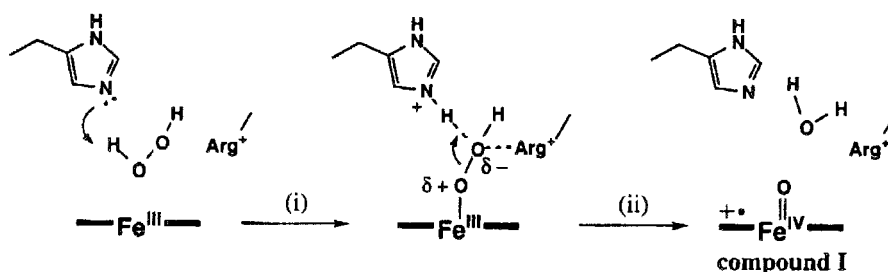
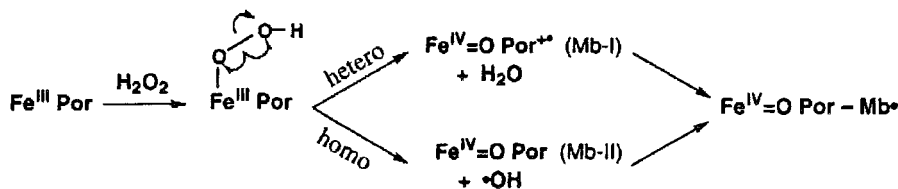


FIG. 1. Superposition of the heme and some selected residues including distal histidines (His-64 in Mb and His-42 in horseradish peroxidase) in crystal structures of sperm whale Mb (ball and stick) and horseradish peroxidase (thin line). A, side view; B, top view. HRP, horseradish peroxidase.

SCHEME II. Proposed reaction scheme of ferric Mb with hydrogen peroxide.



similar distance from the heme iron compared with those in peroxidases, whereas the distal histidine in L29H/H64L Mb is located too far to activate H_2O_2 .

EXPERIMENTAL PROCEDURES

Preparation of Myoglobin Mutants—The expression vectors for wild-type and H64L sperm whale Mb were gifts from John Olson (Rice University) (29, 30). L29H and F43H mutations with new silent *Hin*I and *Pvu*I sites, respectively, were introduced by use of a polymerase chain reaction-based technique. Expression in *Escherichia coli* strain TB-1 and purification were performed as described previously (31). To purified Mb, when necessary, was added ferricyanide for oxidizing ferrous carbon monoxide Mb to the ferric state. The final purified protein was stored at -80°C , except for the L29H/H64L mutant, which was stored at 4°C .

Spectroscopy—Electronic absorption spectra in 50 mM sodium phosphate buffer (pH 7.0) were recorded on a Shimadzu UV-2400 spectrophotometer, and the concentration of the samples was $10\ \mu\text{M}$. ^1H NMR spectra in 0.1 M sodium phosphate buffer (pD 7.0) were recorded at 25°C and 270 MHz on a JEOL EX-270 spectrometer. Chemical shifts were referenced to HDO.

Reactions with Hydrogen Peroxide—All reactions of ferric Mb with H_2O_2 were carried out in 50 mM sodium phosphate buffer (pH 7.0). Formation rates of a ferryl heme in wild-type and F43H/H64L Mb (see also "Results") were determined at 20°C from the decay of absorbance at 407 nm. Bimolecular rate constants were given by the slope of a plot of the observed rates versus H_2O_2 concentration. The amounts of H_2O_2 were kept >10 molar eq over Mb for ensuring the pseudo first-order condition ($[\text{Mb}] = 1.0$ and $0.5\ \mu\text{M}$ for wild-type and F43H/H64L Mb, respectively). Whole spectral changes of rapid reactions were monitored by using a Hi-Tech SF-43 stopped-flow apparatus equipped with an MG 6000 diode array spectrophotometer.

The catalase activity of Mb was measured at 25°C from amounts of

molecular oxygen formed with a Hansatech DW1 oxygen electrode. The reaction mixture contained $10\ \mu\text{M}$ Mb and 1 mM H_2O_2 .

Consumption rates of H_2O_2 by the L29H/H64L and H64L mutants were determined at 20°C as follows. A reaction mixture of $10\ \mu\text{M}$ Mb mutant and $50\ \mu\text{M}$ H_2O_2 was incubated for 5–30 min. During the incubation, to a solution containing a trace amount of horseradish peroxidase ($800\ \mu\text{l}$, pH 5.3) was added $200\ \mu\text{l}$ of the incubated solution and then an excess amount of potassium iodide. The remaining H_2O_2 was quantified from the amounts of triiodide formed using absorbance changes at 353 nm ($\epsilon_{353} = 2.62 \times 10^4\ \text{M}^{-1}\ \text{cm}^{-1}$) (32). Under these conditions, the Mb mutants did not show any considerable spectral change, including absorbance at 353 nm.

Measurements of Oxidation Activities—1-Electron oxidation activities were measured at 20°C in 50 mM sodium phosphate buffer (pH 7.0). At least two experiments were performed for each experimental point. Steady-state kinetic constants for the oxidations of guaiacol and ABTS (2,2'-azino-bis(3-ethylbenzothiazoline-6-sulfonic acid)) were obtained by measuring the initial rates while varying the substrate concentration. A Hanes plot of $[S]/v$ versus $[S]$ was used to estimate the V_{max} and K_m values for the oxidations. The formation rate of the guaiacol oxidation product was determined from the increase in the absorbance at 470 nm using a molar extinction coefficient of $3.8 \times 10^3\ \text{M}^{-1}\ \text{cm}^{-1}$. The 1-ml final assay volume contained $1\ \mu\text{M}$ Mb, $0.2\ \text{mM}$ H_2O_2 , and variable amounts of guaiacol (0.08–2.5 mM). The formation of an ABTS cation radical was monitored at 730 nm, where the absorption of Mb was negligible (19). The absorption coefficient of the ABTS cation radical at 730 nm ($\epsilon_{730} = 1.4 \times 10^4\ \text{M}^{-1}\ \text{cm}^{-1}$) was calculated from that at 415 nm ($3.6 \times 10^4\ \text{M}^{-1}\ \text{cm}^{-1}$) (33). The reaction mixture contained $0.5\ \mu\text{M}$ Mb, $0.2\ \text{mM}$ H_2O_2 , and 20–300 μM ABTS.

Reaction with Cumene Hydroperoxide—A reaction mixture containing $10\ \mu\text{M}$ Mb and $270\ \mu\text{M}$ cumene hydroperoxide was incubated at 20°C in 50 mM sodium phosphate buffer (pH 7.0). Aliquots of the mixture were analyzed by a Shimadzu HPLC system equipped with a

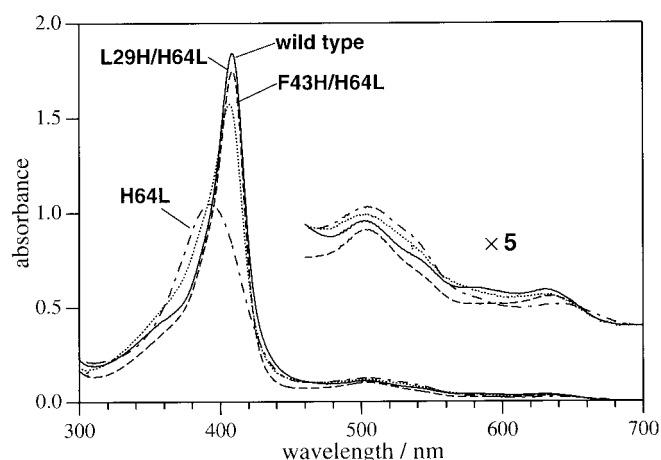


FIG. 2. Absorption spectra of ferric forms of wild-type (—), L29H/H64L (---), F43H/H64L (···), and H64L (- · - ·) Mb in 50 mM sodium phosphate buffer (pH 7.0).

Shimadzu CR-6A data module on a reverse-phase column (GL Sciences Inc., Inertsil ODS). Phenethyl alcohol was employed as an internal standard. The column was eluted with 50% water and 50% methanol at a flow rate of 1.0 ml/min, and the effluent was monitored at 210 nm. Assignment of the components was based on the retention time of authentic samples.

Kinetic Measurements for Association of Azide and Cyanide—The reactions of ferric L29H/H64L and F43H/H64L Mb mutants with azide or cyanide were performed at 20 °C on a Hi-Tech stopped-flow apparatus in 50 mM sodium phosphate buffer (pH 7.0). The kinetic traces at 408 nm were used for determining pseudo first-order rates. The association rate constants were given by the slope of a plot of the observed rates versus azide or cyanide concentration.

X-ray Crystallography—Crystals were grown in the P6 space group using a hanging drop method. 10 μ l of 65 mg/ml HPLC cation ion column-purified protein was mixed with a solution of 3.2 M ammonium sulfate, 20 mM Tris-HCl, and 1 mM EDTA (pH 9.0) to give a final concentration of 2.4–2.6 M ammonium sulfate. The hanging drops were set up at room temperature and incubated at 4 °C. The crystal was mounted, and the diffraction data were collected at room temperature.

Diffraction data were collected on a Rigaku R-AXIS IIC imaging plate system. Data were reduced with XDS and merged using XSCALE. The L29H/H64L data were 98.5% complete in the resolution range 50.0–1.8 Å with $R_{\text{sym}} = 4.8\%$. The F43H/H64L data were 99.0% complete in the resolution range 50.0–1.8 Å with $R_{\text{sym}} = 4.1\%$.

The coordinates of ferric wild-type myoglobin (14) were used as a starting model. The model was refined using X-PLOR (34). An iterative procedure of modifying the model using the molecular graphics program CHAIN (35) followed by Powell minimization, solvent B-factor and occupancy refinement, and individual B-factor refinement for all atoms was repeated until R_{free} was unchanged and no significant differences were observed in electron density maps. The side chain for residues 29 or 43 or 64 were changed only after $|2F_o - F_c|$ and $|F_o - F_c|$ difference Fourier maps indicated clear positions for these altered side chains.

RESULTS

Spectroscopic Features of L29H/H64L and F43H/H64L Mb Mutants—The ferric F43H/H64L and L29H/H64L Mb mutants exhibited absorption spectra similar to that of wild-type Mb (Fig. 2). The Soret maxima is around 408 nm, which indicates a typical hexa-coordinated ferric high-spin heme. The sixth ligand in wild-type Mb is a water molecule stabilized by His-64 through hydrogen bonding (13, 14). Since the loss of water ligation in H64L causes a Soret shift to 393 nm (Fig. 2) (36), the novel histidines in the double mutants appear to stabilize the heme-bound water. The absorption maxima of the ferric CN, ferrous, and ferrous CO forms of the L29H/H64L and F43H/H64L mutants are essentially identical to the corresponding states of wild-type and H64L Mb (data not shown).

Fig. 3 presents hyperfine-shifted ^1H NMR spectra of the ferric forms of wild-type, L29H/H64L, and F43H/H64L Mb at pH 7.0. Four intense peaks in each spectrum are easily assigned

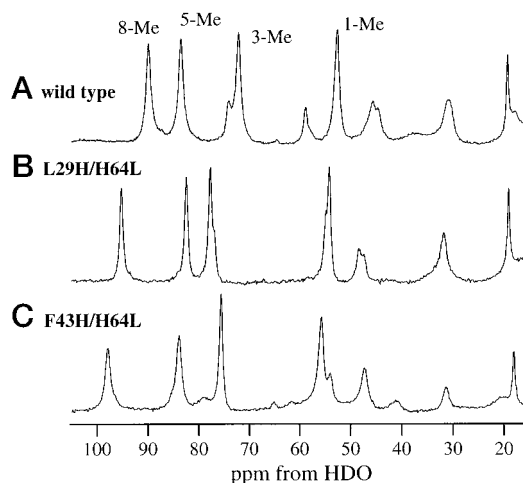


FIG. 3. ^1H NMR spectra of ferric forms of wild-type (A), L29H/H64L (B), and F43H/H64L (C) Mb in 50 mM sodium phosphate buffer (pD 7.0) at 25 °C.

to the heme methyl protons. Although the heme methyl signals of the mutants were slightly downfield-shifted compared with those of wild-type Mb (mean methyl shift: 74.6, 77.3, and 78.3 ppm for wild-type, L29H/H64L, and F43H/H64L Mb, respectively), the double mutations did not greatly alter the whole spectra. A similar shift of the heme methyl protons has been also reported for various His-64 Mb mutants (37, 38). Therefore, the introduction of histidines at positions 29 and 43 does not appear to greatly alter the electronic structures of the ferric hemes.

Reactions of Ferric Myoglobins with H_2O_2 —Ferric wild-type Mb reacted with H_2O_2 to yield a ferryl heme ($\text{Fe}^{\text{IV}}=\text{O}$ Por), equivalent to compound II of peroxidase, paired with a protein radical as reported previously (22–24). The ferryl heme (Mb-II) formation in wild-type Mb showed isosbestic points and obeyed pseudo first-order kinetics. A ferryl porphyrin cation radical ($\text{Fe}^{\text{IV}}=\text{O}$ Por $^+$) for wild-type Mb similar to compound I in horseradish peroxidase (39) has not been observed, probably due to its rapid decay to Mb-II and a protein radical (Scheme II). We have recently shown that the distal histidine (His-64) in wild-type Mb plays a crucial role in destabilizing compound I (40).

The reaction between ferric F43H/H64L and H_2O_2 also resulted in nearly isosbestic conversion to Mb-II (Fig. 4A). The kinetic trace obeyed pseudo first-order kinetics in the incubation with 25 μM H_2O_2 , but not with 500 μM H_2O_2 (Fig. 4B). In the presence of a large amount of H_2O_2 , the apparent deviation of the trace from single exponential curvature reveals a slight accumulation of an intermediate species, which was not clearly observed by varying H_2O_2 concentration, pH, and temperature. The most probable candidate for the intermediate is compound I (Mb-I) because F43H/H64L Mb-I is stable enough for its direct observation when the oxidant is *m*-chloroperbenzoic acid (*m*CPBA) (28). The lesser accumulation of Mb-I with H_2O_2 than *m*CPBA could be attributed to the rapid reduction of Mb-I by H_2O_2 to the ferric state ($2 \times 10^4 \text{ M}^{-1} \text{ s}^{-1}$ for F43H/H64L Mb at 5.0 °C and pH 5.3) (28, 40). In fact, F43H/H64L Mb dismutated H_2O_2 to molecular oxygen and water at a 50-fold higher rate than wild-type Mb (Table I). Therefore, F43H/H64L Mb-I is formed in the reaction with H_2O_2 , and conceivable reactions are summarized in Scheme III.

The reaction rates of ferric wild-type and F43H/H64L Mb with H_2O_2 were determined under the condition where the Mb-I accumulation was negligible. As noted above, there is no kinetic evidence for the formation of wild-type Mb-I. When incubated with a low concentration of H_2O_2 (5.0–20 μM), F43H/H64L Mb-I did not appear to be formed. Plots of the observed

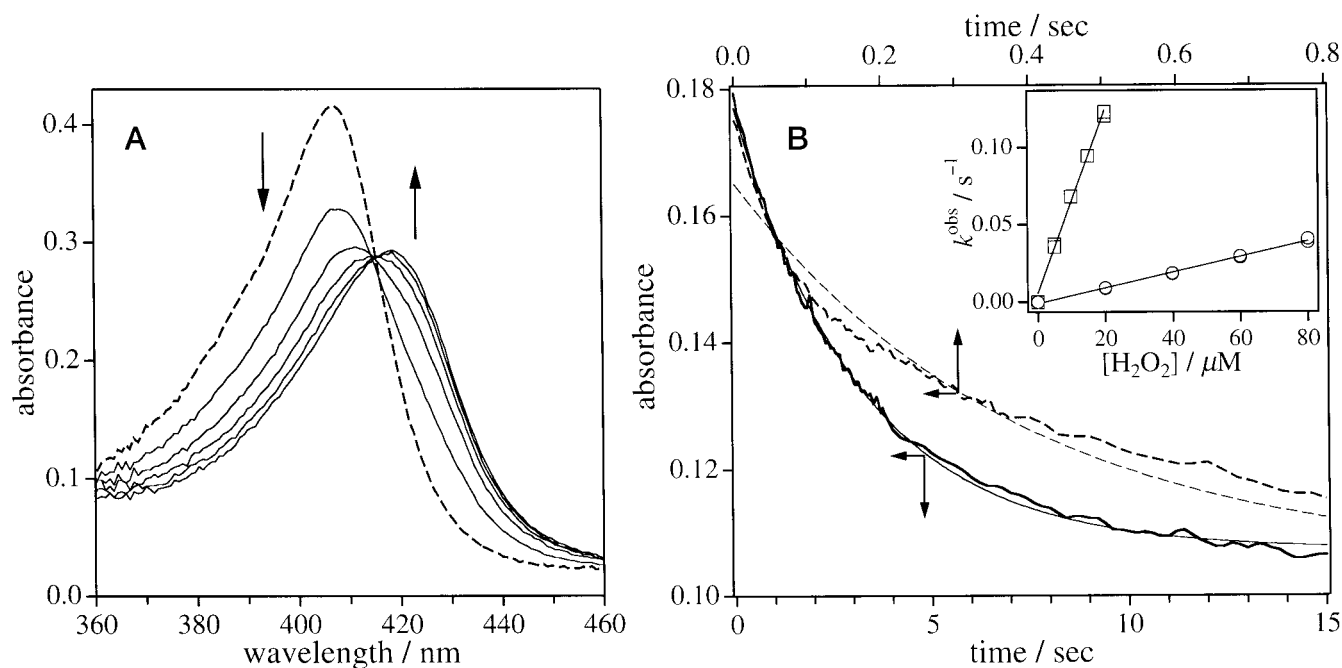


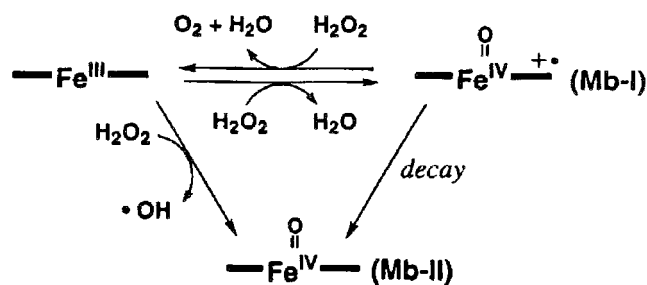
FIG. 4. Spectral change of the F43H/H64L Mb mutant in the reaction with hydrogen peroxide. *A*, whole spectral changes in the Soret region during the incubation with 1 mM H_2O_2 . The spectra were recorded before the reaction (---) and at 0.2–1.8 s after mixing with 0.4-s intervals (—). *B*, time-dependent absorbance change at 407 nm in the presence of 25 μM H_2O_2 (—) and 0.5 mM H_2O_2 (---). The thin lines with each trace represent the best fit to single exponential functions. Inset, hydrogen peroxide concentration-dependent changes in the observed formation rates of Mb-II for wild-type (○) and F43H/H64L (□) Mb. Wild-type and F43H/H64L Mb were present at 1.0 and 0.5 μM , respectively.

TABLE I
Reaction of Mb with hydrogen peroxide at pH 7.0

Mb	Mb-II formation ^a $\text{M}^{-1} \text{s}^{-1}$	O_2 evolution ^b turnover/min
Wild-type	5.1×10^2	1.7
L29H/H64L		8.8
F43H/H64L	5.6×10^3	79

^a The rates were determined at 20 °C.

^b The rates were determined at 25 °C in the presence of 1.0 mM H_2O_2 .



SCHEME III. Plausible scheme for the reaction of ferric Mb with hydrogen peroxide.

formation rates of Mb-II *versus* H_2O_2 concentrations showed good linearity (Fig. 4B, inset). The rate constant for the F43H/H64L mutant is $5.6 \times 10^3 \text{ M}^{-1} \text{ s}^{-1}$, which is 11-fold higher than that for wild-type Mb (Table I). The slight accumulation of F43H/H64L Mb-I with H_2O_2 (Fig. 4A) is consistent with the fact that F43H/H64L Mb-I is more reactive with H_2O_2 than its ferric form. In the incubation with 20 μM H_2O_2 , F43H/H64L Mb-I decayed much faster (9.2 s^{-1} at 5.0 °C and pH 5.3) than its formation or reduction by H_2O_2 (0.1 and 0.4 s^{-1} , respectively).

The ferric L29H/H64L and H64L mutants showed few absorption spectra changes upon the addition of H_2O_2 . Nevertheless, L29H/H64L and H64L Mb slowly consumed H_2O_2 (0.11 and 0.003 min^{-1} , respectively, at $[\text{H}_2\text{O}_2] = 50 \mu\text{M}$) and produced a protein radical as reported for H64V Mb (16). It is likely that

the ferric mutants react with H_2O_2 , but much slower than the decay of the oxidized heme to the ferric state. L29H/H64L Mb-I prepared by *m*CPBA, as well as F43H/H64L Mb-I, was immediately reduced by H_2O_2 to the ferric state, although a requirement for a large excess of *m*CPBA for the Mb-I preparation prevented us from determining the exact reaction rate. The catalase activity of the L29H/H64L mutant was 5-fold higher than that of wild-type Mb (Table I). Because of the mutants being in the ferric form during incubation with H_2O_2 , the reactivity of ferric L29H/H64L and H64L Mb with H_2O_2 can be estimated from the consumption rates of H_2O_2 to be 3–6- and ~100-fold lower than that of wild-type Mb, respectively. The results reveal that the enhancement of H_2O_2 activation by His-64 is more effective than that by His-29.

Oxidation Activities of Wild-type Mb and Its Mutants—1-Electron oxidations of guaiacol and ABTS were examined at pH 7 using H_2O_2 as an oxidant. The initial rates of oxidation by Mb showed hyperbolic dependence on the concentration of the substrates under the conditions employed. Table II summarizes V_{max} and K_m values for the oxidations. F43H/H64L Mb exhibited ~6-fold higher V_{max} values than wild-type Mb both in the guaiacol and ABTS oxidations. In contrast, the L29H/H64L mutant gave one-fourth or less V_{max} values, and we could not find any significant activities for the H64L mutant. The changes in the V_{max} values correlate well with those observed for the reactivities of ferric Mb with H_2O_2 , *i.e.* 11-fold higher *versus* wild-type Mb in F43H/H64L Mb (Table I) and 3–6-fold lower in L29H/H64L Mb. Steady-state absorption spectra of wild-type Mb during the guaiacol oxidation (Fig. 5) indicated that most of wild-type Mb existed as Mb-II in the presence of 40 μM guaiacol, but as the ferric form with 4 mM guaiacol. Therefore, the rate-determining step in the presence of a large excess amount of guaiacol is the reaction of ferric Mb with H_2O_2 .

Reaction with Cumene Hydroperoxide—To examine the capability of the distal histidines as general acids (Scheme I), the reaction of ferric Mb with cumene hydroperoxide (CHP) was performed. The heterolytic O–O bond cleavage of CHP is

TABLE II
1-Electron oxidations catalyzed by Mb at 20 °C and pH 7.0

The concentration of H₂O₂ was 0.20 mM. The units are as follows: V_{max}, nmol of product/nmol of Mb/min; and K_m, μM.

Mb	Guaiacol		ABTS	
	V _{max}	K _m	V _{max}	K _m
Wild-type	6.6	570	26	77
L29H/H64L	1.9	76	3.1	11
F43H/H64L	43	99	150	66

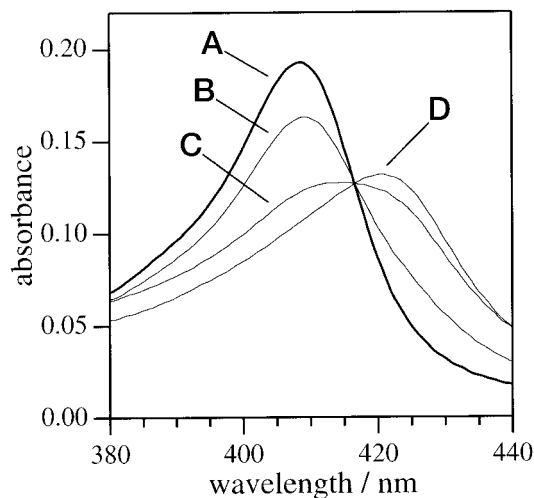
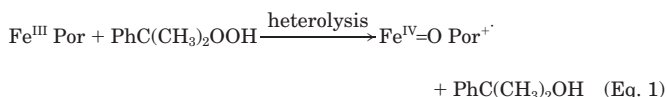
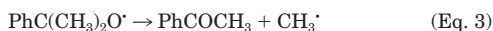
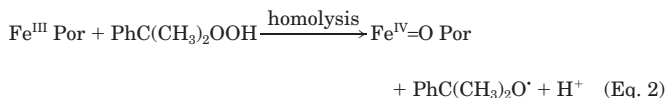


FIG. 5. Steady-state absorption spectra of wild-type Mb during guaiacol oxidation. The spectrum of the ferric state (A) and the steady-state spectra in the presence of 4 mM (B), 400 μM (C), and 40 μM (D) guaiacol are shown.

known to produce compound I (or its equivalent) and cumyl alcohol (Equation 1).



On the other hand, homolysis of the O–O bond gives compound II and the cumyloxy radical, which subsequently eliminates the methyl radical to afford acetophenone (Equations 2 and 3) (41).



The general acid catalyst is expected to selectively enhance heterolysis, which should raise the ratio of heterolysis over homolysis (cumyl alcohol/acetophenone).

As shown in Table IV, the cumyl alcohol/acetophenone ratio was not affected by the H64L substitution, indicating that His-64 in wild-type Mb does not facilitate the heterolysis of the peroxide bond as reported earlier (25). While L29H replacement did not alter the ratio greatly, the F43H/H64L mutant showed a higher cumyl alcohol/acetophenone ratio than the others (Table III). Thus, only His-43 in F43H/H64L Mb is able to facilitate the heterolytic O–O bond cleavage of the heme-bound CHP possibly as a general acid.

Association Rates of Cyanide and Azide—Roles of the distal histidine in H₂O₂ binding (Scheme I) were proposed on the basis of rates of association of cyanide (*k*_{CN}) with the ferric heme iron at pH 7 (Table IV). Most of the cyanide is protonated at neutral pH (*pK*_a ~ 9), and the crucial step for the cyanide association with ferric Mb has been shown to be the deprotonation

TABLE III

Product ratio in the reaction with cumene hydroperoxide

The ratios were determined after 50 min of incubation in 50 mM sodium phosphate buffer (pH 7.0) at 20 °C.

Mb	Cumylalcohol/acetophenone
Wild-type	3.3
H64L	3.3
L29H/H64L	2.8
F43H/H64L	5.4

TABLE IV

Association rate constants of azide and cyanide at 20 °C and pH 7.0

Mb	Azide	Cyanide	Source
	<i>mM</i> ⁻¹ <i>s</i> ⁻¹	<i>mM</i> ⁻¹ <i>s</i> ⁻¹	
Wild-type	2.9	0.32	Ref. 42
H64L	34	0.002	Ref. 42
L29H/H64L	3.5	0.0081	This study
F43H/H64L	31	0.88	This study

nation of HCN in the distal heme pocket (42), as suggested for the binding of H₂O₂ (*pK*_a = 11.6). The 160-fold decrease in the *k*_{CN} for the H64L mutation was attributed to the loss of a general base, His-64 (42). We have also measured the rates of association of azide (*k*_{N₃}) with the ferric heme. In contrast to the cyanide, azide is negatively charged (*pK*_a = 4.5) at neutral pH, and the *k*_{N₃} value was reported to largely depend on the accessibility to the ferric heme center (42). The H64L mutant showed a 12-fold increase in *k*_{N₃} versus wild-type Mb due to the distal heme pocket being more open.

The *k*_{CN} value for F43H/H64L Mb was 2.7- and 440-fold higher than those for wild-type and H64L Mb, respectively (Table IV). Since the H64L and F43H/H64L mutants showed similar *k*_{N₃} values (Table IV), the accessibility to the heme center of the mutants does not seem to greatly differ from each other. Thus, it is likely that His-43, as well as His-64, facilitates cyanide binding as a general base. The *k*_{CN} value for the L29H/H64L mutant was 40-fold lower than that of wild-type Mb, whereas wild-type and L29H/H64L Mb reacted with azide anion at similar rates (Table IV). Thus, His-29 in the L29H/H64L mutant appears to be a less effective base than His-64 and His-43 in supporting cyanide binding.

Crystal Structures of Ferric L29H/H64L and F43H/H64L Mb Mutants—As described above, the L29H/H64L and F43H/H64L mutations to rearrange the distal histidine strongly affected the reactions of Mb with peroxides and anions. To verify the location of the distal histidine, the crystal structures of L29H/H64L and F43H/H64L Mb were determined at 1.8-Å resolution (Fig. 6). The data collection and refinement statistics are listed in Table V. Both Mb mutants exhibited few structural changes upon the double mutations outside the immediate vicinity of the substituted residues (Fig. 6). The distal histidines in the mutants (His-29 in L29H/H64L Mb and His-43 in F43H/H64L Mb) are directed to the heme center. The coordination structures of the ferric heme iron (aquo-hexacoordinations) are consistent with their absorption spectra (Fig. 2). The coordinated water molecules appear to be stabilized by a hydrogen bond with the distal histidine through another water molecule in the active site (Fig. 6). The distance between N^ε of the distal histidine and the ferric heme iron is 5.7 Å in F43H/H64L Mb, which is similar to distances in structurally known peroxidases (5.5–6.0 Å). In contrast, the distal histidine in L29H/H64L Mb is located farther (6.6 Å) from the heme iron than in peroxidases.

DISCUSSION

Roles of the Distal Histidine in the Reaction with Hydrogen Peroxide—We have prepared L29H/H64L and F43H/H64L mu-

FIG. 6. Active-site structures of L29H/H64L (A) and F43H/H64L (B) Mb (gray) superimposed with that of wild-type Mb (black). Balls represent water molecules.

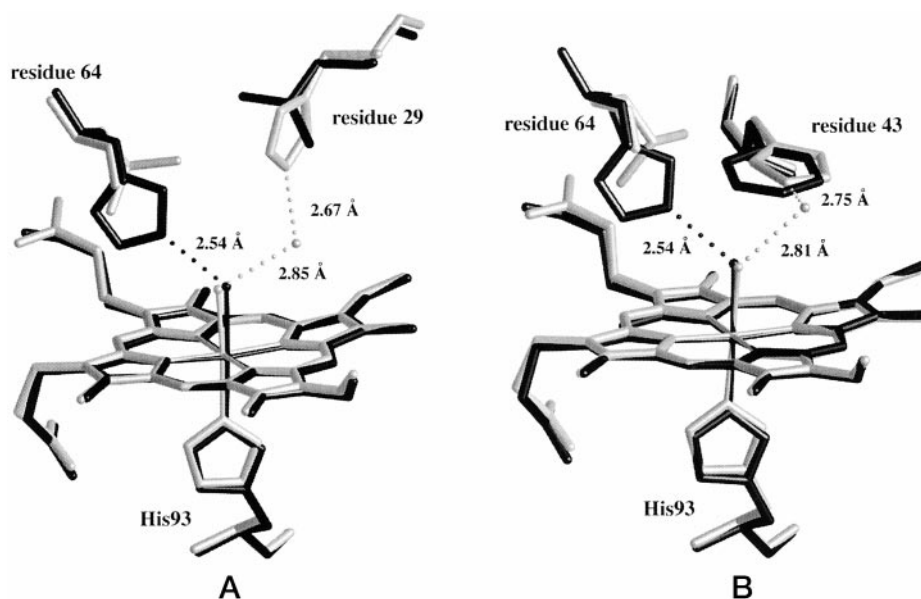


TABLE V
Data collection and refinement statistics for L29H/H64L and F43H/H64L (sperm whale) Mb mutants

	L29H/H64L	F43H/H64L
Unit cell (Å)	$a = b = 91.44$ $c = 45.76$	$a = b = 91.51$ $c = 46.06$
Resolution range (Å)	5.0 to 1.8	5.0 to 1.8
R-factor (%)	16.2	15.3
R _{free} (%)	21.9	19.5
r.m.s. ^a deviations from ideal geometry		
Bond length (Å)	0.010	0.010
Bond angle	1.793°	2.172°
Dihedral angle	18.639°	18.496°
Improper angle	1.416°	1.214°
PDB entry code	10FJ	10FK

^a r.m.s., root mean square; PDB, Protein Data Bank.

tants of sperm whale Mb in which novel distal histidines were designed to be farther from the heme iron than the distal histidine (His-64) in wild-type Mb (Fig. 1). The spectral features of the mutants do not greatly differ from those of wild-type Mb (Figs. 2 and 3), suggesting similar coordination and electronic states of the heme chromophore. The crystal structural analysis revealed that ferric L29H/H64L and F43H/H64L Mb are hexacoordinated with an aquo-ligand as well as ferric wild-type Mb (Fig. 6). The distal histidines in wild-type and double mutant Mb, regardless of their location, are able to stabilize the coordinated water molecule through hydrogen bonding (Fig. 6).

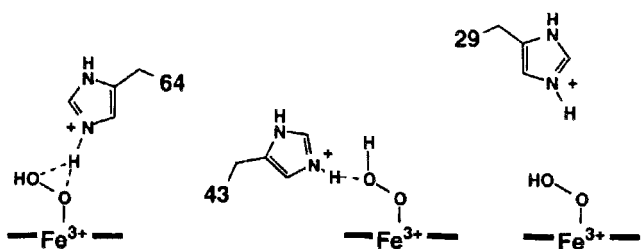
The reactivity of ferric Mb with H₂O₂ is largely dependent on the existence and location of the distal histidine. The ferric H64L mutant with no distal histidine reacted with H₂O₂ ~100 times slower than wild-type Mb, although the single mutant has a vacant sixth coordination site, which seems to be advantageous for H₂O₂ binding. Thus, it is apparent that His-64 in wild-type Mb enhances the reaction with H₂O₂. To estimate the capability of His-64 as a general acid (Scheme I), we have performed the reaction with CHP. The ratio of the heterolytic over homolytic O–O bond cleavage was not affected by the H64L substitution (Table III). A similar result was reported for the H64V mutant using 4-hydroperoxy-4-methyl-2,6-di-*tert*-butylcyclohexa-2,5,dien-1-one (25). Thus, it is unlikely that His-64 functions as a general acid catalyst. To the contrary, His-64 in wild-type Mb has been shown to enhance the association of cyanide with the ferric heme iron presumably by abstracting a proton as a general base (42). Therefore, the role of His-64 should be the enhancement of the binding of H₂O₂ to the

ferric heme, but not the acceleration of the O–O bond cleavage of the heme-bound peroxide (Scheme I).

The distance of His-29 in L29H/H64L Mb from the iron was revealed by x-ray crystallography to be 6.6 Å, which is farther from the heme by 0.6–1.1 Å than in structurally known peroxidases (Figs. 1 and 6A). The ferric L29H/H64L mutant exhibited ~40-fold higher reactivity with H₂O₂ than the H64L mutant, but 3–6-fold lower than wild-type Mb. This indicates that His-29 in the double mutant facilitates the reaction less efficiently than His-64 in wild-type Mb. On the other hand, ferric F43H/H64L Mb has the distal histidine at a similar distance from the heme iron compared with peroxidases (Figs. 1 and 6B) and showed an 11-fold rate increase in the reaction with H₂O₂ versus wild-type Mb (Table I). These results indicate that the proper positioning of the distal histidine is essential for the activation of H₂O₂ by heme enzymes.

The distal histidine in L29H/H64L Mb, as well as that in wild-type Mb, does not appear to work as a general acid catalyst (Table III). Furthermore, His-29 could not efficiently support cyanide binding (Table IV). Therefore, the low reactivity of L29H/H64L Mb with H₂O₂ could be attributed to the poor ability of His-29 as a general base as well as a general acid. In contrast, the F43H/H64L double mutation maintains the high reactivity of ferric Mb with cyanide and raises the heterolytic O–O bond cleavage of CHP (Tables III and IV). We conclude that His-43 serves as a general acid-base catalyst to improve the reactivity with H₂O₂, although it is still less effective than the distal histidine in peroxidase.

Possible interactions between the distal histidines and heme-bound peroxide are depicted in Scheme IV. Our results strongly suggest that the distal histidine in wild-type Mb (His-64) is too close to the heme center to support heterolysis of the peroxide bond to generate compound I. His-64 may interact with both oxygen atoms in the ferric-peroxide complex (Scheme IV). In ferrous oxy-Mb (with structural relevance to the ferric-peroxide complex), heme-bound and terminal oxygen atoms are similar distances from N^ε of His-64 (2.7 and 3.0 Å, respectively) (36). Therefore, although His-64 in oxy-Mb forms a hydrogen bond with the terminal oxygen (43), the iron-bound oxygen atom in the ferric-peroxide complex could also interact with the distal histidine. In fact, the heme-bound water in ferric wild-type Mb makes a direct hydrogen bond with His-64 (13, 14). The interaction of the distal histidine with both oxygen atoms of the iron-bound peroxide (Scheme IV) does not facilitate the charge separation, as suggested for the transition state of the heterolysis (Scheme I).



SCHEME IV. Possible interaction between distal histidines and heme-bound peroxide.

Alternatively, His-43 in F43H/H64L Mb could interact exclusively with the terminal oxygen, whereas His-29 in L29H/H64L Mb could be too far to do so (Scheme IV). These putative structures are supported by changes in the stability of oxy-Mb upon the double mutations. The oxy form of wild-type Mb is stabilized by His-64 and slowly autoxidized to the ferric state (0.05 h^{-1}). The autoxidation of the H64L mutant proceeds much faster (10 h^{-1}) than that of wild-type Mb (44), and L29H/H64L oxy-Mb is too unstable to determine the rate. The results are consistent with the absence of a histidine-oxygen interaction. The modest autoxidation rate for the F43H/H64L mutant (1.3 h^{-1}) is indicative of the hydrogen bond between His-43 and heme-bound oxygen, even though crystal structures of oxy forms of the double mutants are not available at this point due to their instability.

Effects of the Location of the Distal Histidine on Catalytic Activities—The catalytic activities of Mb were measured for the dismutation of H_2O_2 and the 1-electron oxidation of guaiacol and ABTS (Tables I and II). The 1-electron oxidation activities roughly correlate with the reactivities of ferric Mb with H_2O_2 (Tables I and II). On the contrary, the dismutation activity of L29H/H64L Mb was, despite the slower formation of Mb-I, five times higher than that of wild-type Mb (Table I). The 46-fold increase in F43H/H64L *versus* wild-type Mb is greater than the 11-fold improvement in the reactivity of the ferric mutant with H_2O_2 (Table I). The rate-determining step for the 1-electron oxidation is the formation of high valent heme iron as revealed by the steady-state spectra (Fig. 5) in the presence of a large excess amount of the substrates. Since F43H/H64L Mb-I is more reactive with H_2O_2 than its ferric form, the Mb-I formation by H_2O_2 can be involved in the rate-determining step of the H_2O_2 dismutation as in the 1-electron oxidations.

The distinct feature between the 1-electron oxidation and the H_2O_2 dismutation is that Mb-II can oxidize guaiacol and ABTS, but not H_2O_2 . Wild-type Mb-I has not been identified yet, possibly due to its rapid decay to Mb-II and a protein radical. The short lifetime of wild-type Mb-I should cause a significant decrease in the dismutation activity of H_2O_2 , but at most, a 2-fold decrease in the 1-electron oxidation. We have recently shown that His-64 in wild-type Mb plays a crucial role in destabilizing Mb-I (40). The H64L, L29H/H64L, and F43H/H64L mutations prolonged the lifetime of Mb-I enough for its direct observation in the reaction with *m*CPBA (28, 40), suggesting the more efficient oxidation of H_2O_2 by Mb-I in the mutants than in wild-type Mb-I. Therefore, the dismutation activity largely depends on the lifetime of Mb-I as well as the reactivity of ferric Mb with H_2O_2 (Table I).

In summary, we have prepared L29H/H64L and F43H/H64L mutants of sperm whale Mb to clarify the effects of the location of distal histidines on the activation of H_2O_2 . The F43H/H64L mutation causes an 11-fold increase in the activation of H_2O_2 *versus* wild-type Mb presumably because the distance between the distal histidine and the heme iron is similar to that in peroxidases. On the other hand, the distal histidine in L29H/H64L Mb is too far from the iron to enhance the reaction with H_2O_2 . The changes in the reactivity of the mutants with H_2O_2

are rationalized in terms of roles of the distal histidine as a general acid-base catalyst. Whereas His-64 in wild-type Mb functions only as a general base, His-43 in the F43H/H64L mutant is suggested to work as a general acid-base catalyst. It appears that His-29 in the L29H/H64L mutant lacks complete acid-base functionality. Thus, the proper positioning of the distal histidine in heme enzymes is essential for the activation of H_2O_2 especially as a general acid. High catalytic activities are also observed for the F43H/H64L mutant because of the highest reactivity with H_2O_2 and the prolonged lifetime of Mb-I.

REFERENCES

- Edwards, S. L., Raag, R., Wariishi, H., Gold, M. H., and Poulos, T. L. (1993) *Proc. Natl. Acad. Sci. U. S. A.* **90**, 750–754
- Poulos, T. L., Freer, S. T., Alden, R. A., Edwards, S. L., Skogland, U., Takio, K., Eriksson, B., Xuong, N., Yonetani, T., and Kraut, J. (1980) *J. Biol. Chem.* **255**, 575–580
- Patterson, W. R., and Poulos, T. L. (1995) *Biochemistry* **34**, 4331–4341
- Sundaramoorthy, M., Kishi, K., Gold, M. H., and Poulos, T. L. (1994) *J. Biol. Chem.* **269**, 32759–32767
- Kunishima, N., Amada, F., Fukuyama, K., Kawamoto, M., Matsunaga, T., and Matsubara, H. (1996) *FEBS Lett.* **378**, 291–294
- Finzel, B. C., Poulos, T. L., and Kraut, J. (1984) *J. Biol. Chem.* **259**, 13027–13036
- Erman, J. E., Vitello, L. B., Miller, M. A., Shaw, A., Brown, K. A., and Kraut, J. (1993) *Biochemistry* **32**, 9798–9806
- Newmyer, S. L., and Ortiz de Montellano, P. R. (1995) *J. Biol. Chem.* **270**, 19430–19438
- Rodriguez-Lopez, J. N., Smith, A. T., and Thorneley, R. N. F. (1996) *J. Biol. Inorg. Chem.* **1**, 136–142
- Poulos, T. L., and Kraut, J. (1980) *J. Biol. Chem.* **255**, 8199–8205
- Vitello, L. B., Erman, J. E., Miller, M. A., Wang, L., and Kraut, J. (1993) *Biochemistry* **32**, 9807–9818
- Rodriguez-Lopez, J., Smith, A., and Thorneley, R. (1996) *J. Biol. Chem.* **271**, 4023–4030
- Takano, T. (1977) *J. Mol. Biol.* **110**, 537–568
- Phillips, G. N., Jr., Arduini, R. M., Springer, B. A., and Sligar, S. G. (1990) *Proteins Struct. Funct. Genet.* **7**, 358–365
- Ortiz de Montellano, P. R., and Catalano, C. E. (1985) *J. Biol. Chem.* **260**, 9265–9271
- Rao, S. I., Wilks, A., and Ortiz de Montellano, P. R. (1993) *J. Biol. Chem.* **268**, 803–809
- Adachi, S., Nagano, S., Ishimori, K., Watanabe, Y., Morishima, I., Egawa, T., Kitagawa, T., and Makino, R. (1993) *Biochemistry* **32**, 241–252
- Matsui, T., Nagano, S., Ishimori, K., Watanabe, Y., and Morishima, I. (1996) *Biochemistry* **35**, 13118–13124
- Everse, J., Johnson, M. C., and Marini, M. A. (1994) *Methods Enzymol.* **231**, 547–561
- Nagano, S., Tanaka, M., Ishimori, K., Watanabe, Y., and Morishima, I. (1996) *Biochemistry* **35**, 14251–14258
- Mukai, M., Nagano, S., Tanaka, M., Ishimori, K., Morishima, I., Ogura, T., Watanabe, Y., and Kitagawa, T. (1997) *J. Am. Chem. Soc.* **119**, 1758–1766
- King, N. K., and Winfield, M. E. (1963) *J. Biol. Chem.* **238**, 1520–1528
- Yonetani, T., and Schleyer, H. (1967) *J. Biol. Chem.* **242**, 1974–1979
- Fenwick, C. W., and English, A. M. (1996) *J. Am. Chem. Soc.* **118**, 12236–12237
- Allentoff, A. J., Bolton, J. L., Wilkiss, A., Thompson, J. A., and Ortiz de Montellano, P. R. (1992) *J. Am. Chem. Soc.* **114**, 9744–9749
- Gajhede, M., Schuller, D. J., Henriksen, A., Smith, A. T., and Poulos, T. L. (1997) *Nat. Struct. Biol.* **4**, 1032–1038
- Ozaki, S., Matsui, T., and Watanabe, Y. (1996) *J. Am. Chem. Soc.* **118**, 9784–9785
- Ozaki, S., Matsui, T., and Watanabe, Y. (1997) *J. Am. Chem. Soc.* **119**, 6666–6667
- Springer, B. A., and Sligar, S. G. (1987) *Proc. Natl. Acad. Sci. U. S. A.* **84**, 8961–8965
- Carver, T. E., Rohlfs, R. J., Olson, J. S., Gibson, Q. H., Blackmore, R. S., Springer, B. A., and Sligar, S. G. (1990) *J. Biol. Chem.* **265**, 20007–20020
- Springer, B. A., Egeberg, K. D., Sligar, S. G., Rohlfs, R. J., Mathews, A. J., and Olson, J. S. (1989) *J. Biol. Chem.* **264**, 3057–3060
- Ramette, R. W., and Sandford, R. W. J. (1965) *J. Am. Chem. Soc.* **87**, 5001–5005
- Ozaki, S., and Ortiz de Montellano, P. R. (1995) *J. Am. Chem. Soc.* **117**, 7056–7064
- Brunger, A. (1992) *X-PLOR Version 3.1 Manual*, Yale University Press, New Haven, CT
- Sack, J. S. (1988) *J. Mol. Graph.* **6**, 244–245
- Quillin, M. L., Arduini, R. M., Olson, J. S., and Phillips, G. N., Jr. (1993) *J. Mol. Biol.* **234**, 140–155
- Rajaraman, K., La Mar, G. N., Chiu, M. L., Sligar, S. G., Singh, J. P., and Smith, K. M. (1991) *J. Am. Chem. Soc.* **113**, 7886–7892
- Ikeda-Saito, M., Hori, H., Andersson, L. A., Prince, R. C., Pickering, I. J., George, G. N., Sanders, C. R., II, Lutz, R. S., McKelvey, E. J., and Matterna, R. (1992) *J. Biol. Chem.* **267**, 22843–22852
- Dunford, H. B., and Stillman, J. S. (1987) *Coord. Chem. Rev.* **19**, 187–251
- Matsui, T., Ozaki, S., and Watanabe, Y. (1997) *J. Biol. Chem.* **272**, 32735–32738
- Meehan, E. J., Kolthoff, I. M., Auerbach, C., and Minato, H. (1961) *J. Am. Chem. Soc.* **83**, 2232–2234
- Brancaccio, A., Cutruzzola, F., Allocatelli, C. T., Brunori, M., Smerdon, S. J., Wilkinson, A. J., Dou, Y., Keenan, D., Ikeda-Saito, M., Brantley, R. E., Jr., and Olson, J. S. (1994) *J. Biol. Chem.* **269**, 13843–13853
- Phillips, S. E., and Schoenborn, B. P. (1981) *Nature* **292**, 81–82
- Brantley, R. E., Jr., Smerdon, S. J., Wilkinson, A. J., Singleton, E. W., and Olson, J. S. (1993) *J. Biol. Chem.* **268**, 6995–7010